Mem. S.A.It. Vol. 76, 945

Memorie della

A study of the photometrical properties of solar magnetic features by numerical simulation

S. Criscuoli[1,2,3] and M. P. Rast[3]

[1] Dipartimento di Fisica, Università di Roma "Tor Vergata", Via della Ricerca Scientifica 1, I-00133 Roma, Italia
[2] INAF - Osservatorio astronomico di Roma , Via Frascati 33, I-00040, Monte Porzio Catone, Italia
[3] High Altitude Observatory, NCAR, Boulder, CO 80307-3000, USA
e-mail: serenac@hao.ucar.edu, mprast@ucar.edu

Abstract.
Existing numerical simulations reproduce many of the observed geometrical and photometrical characteristics of solar magnetic structures. Nonetheless, some quite fundemental properties, such as network center-to-limb variation and facular contrast, which depend on both the structure's size and magnetic field intensity, are still only partially understood. In order to investigate these problems, we have developed a radiative transfer code, based on the short characteristics method, that enables detailed study of the radiative properties of individual magnetic flux tubes and unresolved aggregates of them.

Key words. Sun: flux tube - Sun: MHD models - Sun: faculae, plage

Knowledge of the dynamics and organization of magnetic structures in the solar photosphere, as determined by the interaction of magnetic field with surrounding convective plasma, is fundamental to the understanding of broader solar phenomena such as flare initiation, chromospherical and coronal heating, and solar irradiance variation. To investigate the radiative properties of individual magnetic flux tubes and unresolved aggregates of them, we have developed a radiative transfer code based on the short-characteristics method. This code, when coupled with a pre-existing magnetohydrodynamics code, will also allow study of the interaction of magnetic fields with convection and thus the investigation of fluxtube dynamics and energy balance.

Send offprint requests to: Serena Criscuoli e-mail: serenac@hao.ucar.edu

1. The model and the method

We consider a plane-parallel atmosphere, infinite in extent and with constant properties along one Cartesian direction, as illustrated by Fig. 1. The approximations of local thermodynamic equilibrium and gray atmospheric opacity are assumed, and the radiative intensity in a given direction at each point in the domain is computed by a short-characteristics integration of the transfer equation (1). The radiative flux is then estimated via a numerical quadrature scheme. Because of symmetry, these intrinsically three-dimensional calcula-

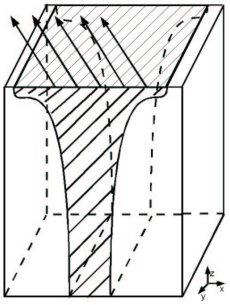

Fig. 1. Spatial domain is a 3D plane parallel atmosphere, infinite and constant along direction y and periodic along x.

tions can be performed by projection of the ray paths onto a two-dimensional spatial grid.

The intensity along a particular direction ω is determined by solving the radiative transfer equation:

$$\frac{\mathrm{d}I(\omega)}{\mathrm{d}\tau} = I(\omega) - S \tag{1}$$

where τ is the optical depth and S is the source function. The short-characteristics technique (Mihalas et al. 1978) allows numerical calculation of the intensity on a spatial grid given the source function S, the opacity function α in the domain, and a boundary condition. Suppose the intensity is known at a point M of the grid in Fig. 2, then the formal solution of Eq. 1 gives the intensity at point O:

$$I_O(\omega) = I_M \mathrm{e}^{-\Delta\tau_M} + \\ + \int_O^{\Delta\tau_M} \mathrm{d}t \;\; S(t)\mathrm{e}^{(-\Delta\tau_M + t)} \tag{2}$$

where

$$\Delta\tau = \int_{s_M}^{s_O} \alpha(s)\mathrm{d}s \tag{3}$$

and s is the path length along the ray direction. The integrals in Eqs. 2 and 3 are estimated by a polynomial expansion (generally at second order) around point O of the integrand functions. The evaluation of integrands at points P and M, that don't belong to the grid, and

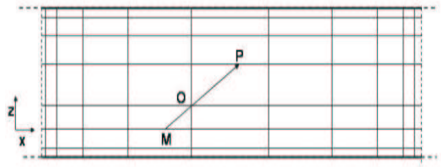

Fig. 2. A Ray propagates on a 2D cartesian grid. Boundary conditions are imposed at top or at bottom according to propagation direction.

the determination of the intensity at point M, are done by interpolation. Given a boundary condition, the intensity is evaluated at each point of the grid row by row starting from the first column for which point M belongs to the previous row. Periodic conditions are imposed on vertical boundaries so that the intensity has the same value at the first and last point of any given row.

2. Tests results

In order to evaluate the short-characteristics method for speed and accuracy, we have performed several tests. These include comparison of results obtained with integration and interpolation schemes of different order, as well as those obtained with schemes of the same order on grids of differing spatial resolution or with rays sampling differing propagation directions. As an example we present in Fig. 3*A-C* results obtained with a second order scheme applying a delta function, a Gaussian or a step function intensity perturbation respectively to the lower boundary of the domain, and propagating it through a vacuum (α=0, S=0) interior. This 'search beam' test elucidates interpolation effects. Intensity profiles at top of the domain (lower panels) as well as field intensity images (upper panels) show that the beam is broadened and attenuated, with the peak asymmetrically shifted. These effects have been studied for first and second order interpolation schemes, and we have found that while first order schemes are dispersive, they conserve energy, while second order schemes do not. Furthermore, these interpolation errors as well as numerical integration errors are more pro-

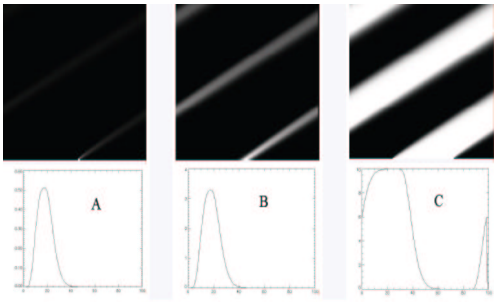

Fig. 3. Ray intensity on the domain (upper panels) and intensity profiles at the top of the grid (lower panels) for three different boundary conditions at the bottom: A)delta function; B)Gaussian function; C)step function.

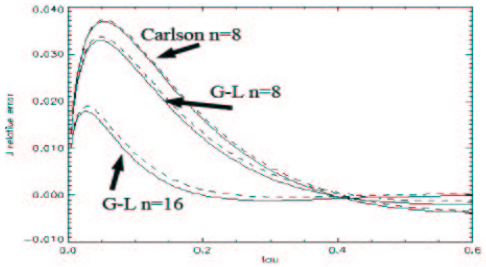

Fig. 4. Relative error in the evaluation of mean intensity integral J as a function of the optical depth in the case of a Lambert radiator. Continuous line: integrand function (intensity field) is an analytical function. Dashed line: integrand function is estimated by our radiative transfer code. Carlson and G-L schemes results are comparable when the number of points per octant (10 in this case, corresponding to n=8) is the same. Even though reduced, maximum relative error is still 2% with n=16 (144 points per octant)in G-L scheme, indicating the necessity of a higher order scheme.

nounced for shallow ray angles. This results from both the increased total path length and the effectively coarser grid sampled by an inclined ray. Finally, no spurious negative intensities, observed for second order interpolations (Auer & Paletou 1994), are present, since *monotonicity* is demanded (van Leer 1977) when using this scheme.

Two quadrature schemes for flux evaluation have been tested. The Carlson scheme is that most often used in previous studies (Mihalas et al. 1978; Bruls et al. 1999). Unfortunately it allows a limited number of points per octant. This limitation is significant (below), and we circumvent it by adopting a Gauss Legendre quadrature for polar angles and a trapezoidal for azimuthal angles (G-L scheme in the following). In both Carlson and G-L schemes a given order n corresponds to $n(n+2)/2$ points per octant. Figure 4 plots the error in the mean intensity integral evaluation for a zero order Eddington-Barbier atmosphere (Lambert radiator). Results obtained with the two schemes are comparable when using the same number of points per octant, but the maximum relative error, even when employing an eight order scheme, is more than 3% in both cases. Doubling the quadrature order in G-L evaluation leads to a maximum relative error of about 2%, indicating that, even for such a simple atmospheric model, a significant number of points per octant is required for a reasonable accuracy.

We are currently evaluating other more symmetrical quadrature schemes which can be extended to very high orders. Some of these are borrowed from quite different disciplines (Steinacker et al. 1996; Górski et al. 2005).

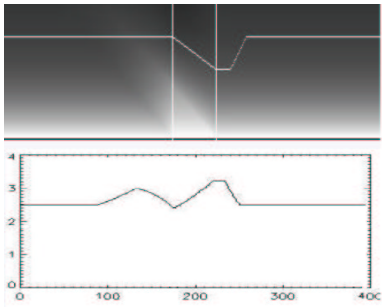

Fig. 5. Intensity field (upper panel) and intensity profile (lower panel) at τ=1 observed at 45° respect to z axis in the Lambert radiator approximation. In upper panel the flux tube (delimited by vertical lines) and τ=1 surface are also illustrated. A flux-tube observed at this angle might look like two different structures.

3. Present and future work

As a first application, we have considered a model atmosphere in which the presence of magnetic field is mimicked by imposing lower α and S functions in a limited region. Intensity profiles at τ=1 surface for several view angles have been analyzed. As an example, Fig. 5 shows the intensity field (upper panel) and the corresponding intensity profile at τ=1 surface (lower panel) obtained for a Lambert radiator atmosphere in which the opacity and the Source function were set to zero in the central region. This extremely simple model already shows some properties in common with observations of magnetic structures observed in very high resolution G-band images. As in the more realistic simulations of Steiner (2005), we obtain that the tube, when observed at certain angles, can produce an area of mixed contrast, thus creating the apparent three dimensionality observed by Lites et al. (2004). The positive contrast peak is generally shifted with respect to the tube center and the non zero contrast area is broader than the tube size. We also notice that, as shown in Fig. 5, more than one intensity peak can appear. These effects raise interesting observational questions, like the correspondence between magnetograms and filtergrams or broadband images, which will be the subject of future investigation. With these aims in mind we are developing a more realistic model with energy balance and pressure equilibrium taken into account, along with opacity stratification.

Acknowledgements. We are grateful to R. Manso Sainz for the helpful discussions and suggestions. The National Center for Atmospheric Research is sponsored by the National Science Foundation.

References

Auer, L.H., & Paletou, F. 1994, A&A, 284, 675
Bruls, J.H.M.J., Vollmöller, P., & Schüssler M. 1994, A&A, 284, 675
Górski, K.M, Hivon, E., Banday, A.J, Hansen, F.K., Reinecke, M., & Bartelmann, M. 2005, ApJ, 622, 759
Lites, B.W., Scharmer, G.B., Berger, T.E., & Title, A.M. 2004, Sol. Phys., 221, 65
Mihalas, D., Auer, L., & Mihalas, B.R. 1978, ApJ, 220, 1001
Steinacker, J., Thamm, E., & Maier, U. 1996, JQSRT, 56, 97
Steiner, O. 2005, A&A, 430, 691
van Leer, B. 1977, J.Comp.Phys., 23, 276